DOI: 10.1002/cphc.201000351

Multilayer Substrate-Mediated Tuning Resonance of Plasmon and SERS EF of Nanostructured Silver**

Lian C. T. Shoute*[a]

A thin-film of dielectric on a reflecting surface constituting a multilayer substrate modulates light intensity due to the interference effect. A nanostructure consisting of randomly oriented silver particles of different shapes, sizes, and interparticle spacings supports multiple plasmon resonances and is observed to have a broad extinction spectrum that spans the entire visible region. Combining the two systems by fabricating the nanostructure on the thin-dielectric film of the multilayer substrate yields a new composite structure which is observed to modulate both the extinction spectrum and the SERS EF (surface enhanced Raman scattering enhancement factor) of the nanostructure as the thickness of the thin-film dielectric is varied. The frequency and intensity of the visible extinction spectrum vary dramatically with the dielectric thickness and in the intermediate thickness range the spectrum has no visible band. The SERS EF determined for the composite structure as a function of the thin-film dielectric thickness varies by several orders of magnitude. Strong correlation between the magnitude of the SERS EF and the extinction intensity is observed over the entire dielectric thickness range indicating that the extinction spectrum corresponds to the excitation of the plasmon resonances of the nanostructure. A significant finding which has potential applications is that the composite structure has synergic effect to boost SERS EF of the nanostructure by an order of magnitude or more compared to the same nanostructure on an unlayered substrate.

1. Introduction

Detection and identification of a trace quantity of molecules in a monolayer adsorbed on the surface of a substrate or molecules attached to the tip of an electrode are critical to the development of emerging functional devices such as molecular electronic devices.[1–4] In situ characterization[5,6] of the devices can provide information on the function of the molecules and allows establishment of a structure–function relationship, consequently leading to the rational design of molecular electronic devices. Raman spectroscopy is a powerful noninvasive analytical tool for chemistry and biology because it provides fingerprint information of the molecules in the form of sharp vibrational bands of the functional groups. However, normal nonresonant Raman has ultralow sensitivity, that is, 10^{14} times less sensitive than fluorescence[7] and hence is not sensitive enough to detect a monolayer of molecules on surfaces. Surface enhanced Raman scattering (SERS) from molecules in close proximity to a metal nanostructure have been extensively investigated[8,9] to overcome this deficiency and now single-molecule detection has been achieved.[10,11]

SERS effect arises predominantly from the inordinate amplification of electromagnetic field at or near the surface of a noble metal nanostructure due to the excitation of localized surface plasmon resonance (LSPR) by the incident electric field.[12–14] Maximum SERS enhancement for a given nanostructure can be achieved when both the incident and the Raman scattered electric fields are maximally enhanced.[15,16] Hence, tuning the LSPR frequency to overlap the Raman excitation and emission frequencies is a core issue in SERS research. It is important to note that analyte–metal charge-transfer formation can lead to a Raman signal enhancement from the resonance Raman effect in a mechanism that is often termed as the chemical mechanism of SERS.[17,18]

The excitation of the LSPR of noble metal nanoparticles results in intense UV/Vis extinction due to absorption and scattering of the incident light and leads to a spectrum not present in the bulk metal. The wavelength of the LSPR extinction maximum (LSPR λ_{max}) is determined by the dielectric properties of the metal nanoparticles, their size and shape, interparticle interactions, and the dielectric constant of the surrounding medium. An intuitive approach to understanding the plasmon resonance of a complex nanostructure is plasmon hybridization, where, the plasmon resonance of a nanostructure with complex geometry can be constructed from the interactions or mixing of the plasmon resonances of simple primary structures.[19,20] Tuning of the LSPR λ_{max} is often achieved by changing the nanoparticle shape and size. For spherical nanoparticles, relatively small shifts of the LSPR λ_{max} can be achieved by changing the size of the nanoparticle.[21,22] However, for shapes other than the sphere, the particle size has a strong effect on the LSPR λ_{max}.[23,24] For example, changing the size of triangular shaped nanoparticles allows the LSPR λ_{max} to be tuned from

[a] Dr. L. C. T. Shoute
Department of Chemistry
National Institute for Nanotechnology
University of Alberta, Edmonton, Alberta T6G 2M9 (Canada)
Fax: (+1) 780-641-1601
E-mail: lshoute@ualberta.ca

[**] SERS EF: Surface-enhanced Raman scattering enhancement factor.

Supporting information for this article is available on the WWW under http://dx.doi.org/10.1002/cphc.201000351.

the visible to mid infrared.[23,24] Core–shell structures[23,25] and nanoparticles with different shapes such as rods,[26] stars,[27] cubes,[28] rings,[29] and so on, have been prepared to tune the plasmon resonance.

Silver island film (AgIF) obtained by vapor deposition of Ag on a multilayer substrate, consisting of a spacer dielectric layer with a bottom reflecting layer, has been demonstrated to modulate the color and SERS EF (surface enhanced Raman scattering enhancement factor) when the spacer layer thickness is varied.[30–34] We[35] and others[32–34] have attributed the modulation of the SERS EF by the spacer thickness of the multilayer substrate as due to interference effects. However, these studies did not address several important issues, such as, the nature and correlation of the color of the substrate with the SERS EF. Recently, there has been renewed interest in systems composed of metal nanostructure-continuous metal film structures separated by a spacer dielectric gap, because they serve as models for metal–insulator–metal sub-wavelength waveguides,[36–38] for understanding the plasmon resonance frequencies arising from LSPR–surface plasmon polariton (SPP) interactions,[39–42] and as a robust and easy to fabricate SERS substrates with high signal amplification. Substrates with this configuration have been theoretically predicted to have SERS EF[43–45] as high as 10^{11}. Herein, it is demonstrated that multilayer substrate tunes the plasmon resonances of AgIF and consequently modulates the SERS EF. A significant finding which has potential applications in SERS development is that, the multilayer substrate used as an active support for plasmonic nanostructure provides additional 10 fold or more enhancement of the SERS EF compared to the same nanostructure supported on an unlayered substrate.

2. Results and Discussion

Figure 1 ashows an absorption spectrum obtained in transmission mode for a 6 nm AgIF on a glass slide. The spectrum is broad with a maximum at 475 nm and spans the entire visible range due to contributions from the excitations of multiple plasmon resonances of Ag nanoparticles of different shapes, sizes, orientations, and interparticle separations. The extinction spectra obtained in the reflectance mode for a multilayer substrate, Ag(100)/SiO_2(38), before (Figure 1 b) and after (Figure 1 c) deposition of 6 nm AgIF is also shown in Figure 1. The highly reflective substrate develops intense color upon the deposition of 6 nm AgIF, indicating excitation of the LSPR of the AgIF. In addition, the peak extinction intensity is ~5 times more than that of 6 nm AgIF on glass.

As shown in Scheme 1, the color of the multilayer substrate with the 6 nm AgIF is strongly modulated by the spacer SiO_2 thickness. When the spacer SiO_2 thickness is varied in the range 18–390 nm while the reflecting Ag(100) and Ag(6) layers are kept constant, the extinction spectrum varies significantly, as shown in Figure 2. In the 18–46 nm SiO_2 thickness range, the extinction spectrum has an intense peak in the visible region and shifts to a longer wavelength with increasing SiO_2 thickness (Figure 2 a). Similar spectra with an intense visible peak that red shifts with increasing SiO_2 thickness were observed for the SiO_2 thickness range 230–390 nm (Figure 2 b). In contrast, the extinction spectrum changes dramatically with SiO_2 thickness between 60 and 218 nm (Figure 2 c) and in the 129–153 nm spacer thickness region the extinction spectrum

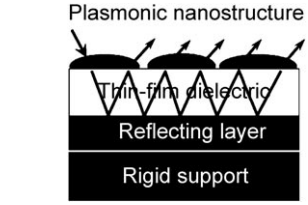

Scheme 1. Schematics of composite multilayer substrate consisting of a silver nanostructure on thin-film dielectric or specifically the spacer SiO_2 layer. The reflecting layer is an optically thick 100 nm silver layer deposited on a 0.5 mm thick silicon wafer with thermal oxide acting as the rigid support. The incident light undergoes multiple internal reflections within the dielectric layer. Note that for quartz, the critical angle and Fresnel coefficient (glass–air) are 40.2° and 0.11 respectively for TE polarized 514.5 nm light. Increased reflectivity due to the deposition of AgIF on multilayer substrate is expected to facilitate multiple internal reflections.

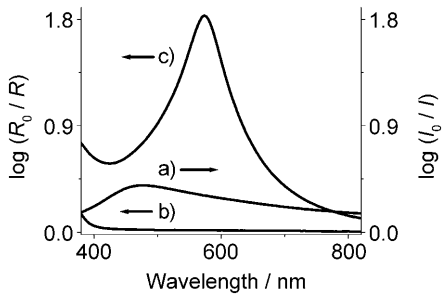

Figure 1. Absorption spectrum [log(I_o/I)] of 6 nm AgIF on glass (a). Transversed electric (TE) polarized extinction [log(R_o/R)] spectra of a Ag(100)/SiO_2(38) substrate, which has 38 nm SiO_2 layer thickness, before (b) and after (c) deposition of 6 nm AgIF.

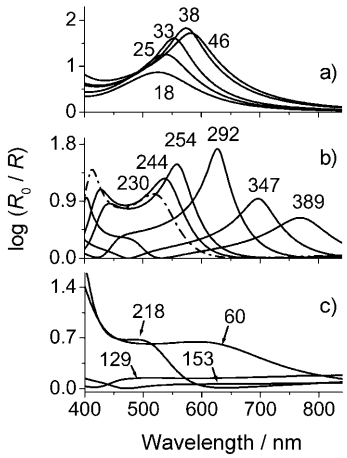

Figure 2. TE polarized extinction spectra of Ag(100)/SiO_2(xx)/Ag(6) multilayer substrates with three SiO_2 thickness ranges: a) 18–46 nm SiO_2, b) 230–389 nm SiO_2, and c) the intermediate 60–218 nm SiO_2 thickness. The number adjacent to the extinction spectrum corresponds to SiO_2 thickness in nm.

has no peak in the visible region. In order to understand the nature and origin of the extinction spectra we have recorded the extinction spectrum of each substrate before depositing 6 nm AgIF. As shown in Figure 1 b, the extinction spectrum due to Ag(100)/SiO_2(38) without AgIF is weak and has no peak in the visible region. However, in the 230–390 nm region the spectrum has a weak peak which shifts with SiO_2 thickness as shown in Figure S1 a–c (Supporting Information). The extinction spectra of the multilayer substrates without AgIF are blue shifted, 1 to 2 orders of magnitude less intense, and are strongly correlated to the spectra with AgIF. These results indicate that interference effect in the spacer layer of the multilayer substrate modulates the extinction spectrum of AgIF.[35]

Important questions studied here include how the extinction spectrum of the multilayer substrate relates to the LSPR of AgIF and whether the multilayer substrate tunes the LSPR wavelength of AgIF. This question can be addressed according to the electromagnetic mechanism[12–16] of SERS by the correlation between extinction and the SERS EF. The electromagnetic mechanism of SERS predicts that the SERS EF should correlate with the observed extinction if it is due to the excitation of LSPR, since both are mediated by the LSPR.[12–16] To investigate such a correlation, we determined the SERS EFs of 4-nitroazobenzene (NAB) chemisorbed on AgIF-multilayer substrate systems as shown in Figures 1and 2.

The Raman spectrum of 0.014 M NAB in dimethylsulfoxide solution and the SERS spectrum of a monolayer of 4-nitroazobenzene (NAB) chemisorbed on the surface of AgIF-multilayer substrate system is presented in Figure 3. The details of the

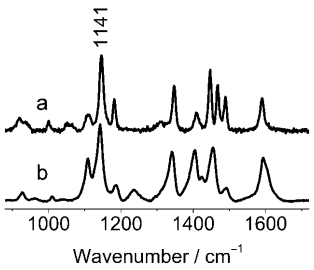

Figure 3. Raman spectra of NAB a) in DMSO solution and b) on a AgIF multilayer composite substrate.

NAB Raman band assignments can be found in an earlier report.[6] The SERS EFs of NAB adsorbed on AgIF surface of the multilayer substrates were determined as described earlier.[35] Briefly, the Raman peak intensity of 1141 cm^{-1} band of NAB in solution (I_{soln}) and of NAB on the AgIF surface of the multilayer substrates (I_{surf}) were experimentally measured at 514.5 nm excitation. The SERS EFs are calculated from the number of molecules probed by the Raman excitation laser in solution (N_{soln}) and on the AgIF surface (N_{surf}) of the multilayer substrate using Equation (1):

$$\text{SERS} \quad \text{EF} = \frac{I_{surf}}{I_{soln}} \times \frac{N_{soln}}{N_{surf}} \qquad (1)$$

The electromagnetic contribution to the SERS enhancement at or near the metal nanostructure is related to the incident excitation and the amplified local electric fields due to the excitation of LSPR as in Equation (2):

$$\text{SERS} \quad \text{EF} = \left|\frac{E_{local}(\nu_{ex})}{E_{in}(\nu_{ex})}\right|^2 \times \left|\frac{E_{local}(\nu_{Ram})}{E_{in}(\nu_{Ram})}\right|^2 \qquad (2)$$

where, $E_{local}(\nu_{ex})$ and $E_{local}(\nu_{Ram})$ are the local electric fields at the excitation and Raman frequencies at or near the metallic nanostructure due to the excitation of LSPR, and $E_{in}(\nu_{ex})$ and $E_{in}(\nu_{Ram})$ are the corresponding electric fields in the absence of the metal nanostructure. This equation shows that the SERS EF is a measure of the local field enhancement at or near the surface of the nanostructure and occurs as a result of the excitation of LSPR. The extinction spectrum represents the LSPR frequencies of the nanostructure. The relationship between the extinction and SERS EF has been experimentally demonstrated by van Duyne et al.[15,16] from the correlation between extinction spectra and wavelength scanned surface-enhanced Raman excitation profiles of a number of nanostructures fabricated by nanosphere lithography. They showed that the SERS EF is maximized when the incident and the Stokes shifted Raman scattered light are equally enhanced and this occurs when the extinction maximum is located midway between the incident and the Raman scattered frequencies that is, at $(\nu_{ex} + \nu_{Ram})/2$. Thus, the SERS EF can be correlated with the extinctions at both the excitation and the Raman scattered frequencies, and the extinction at $(\nu_{ex} + \nu_{Ram})/2$ should track the SERS EF excitation profile.

The SERS EFs were determined by exciting with transverse electric (TE) polarized 514.5 nm laser as a function of SiO_2 spacer thickness of the multilayer substrate, Ag(100)/SiO_2(variable)/Ag(6), while maintaining the AgIF film thickness constant at 6 nm. Note that the plot of SERS EF versus AgIF thickness for the multilayer substrate with constant spacer thickness has a maximum at ~6 nm AgIF thickness (see Figures 5 b and 6 b), hence 6 nm AgIF is used in all subsequent studies. The plot of SERS EF versus SiO_2 thickness presented in Figure 4 a shows two peaks and a valley, a trend that can be expected from interference effect in stratified layers. The two peaks have similar SERS EF of $\sim 1.1 \times 10^7$ and occur at ~38 and ~240 nm spacer SiO_2 thicknesses. The valley or minimum between the two maxima is located at ~150 nm spacer SiO_2 thickness and has dramatically lower SERS EF of 4.8×10^4. These results indicate that multilayer substrates can have a dramatic effect on the SERS EF, with the spacer thickness modulating the SERS EF by a factor of ~230.

To correlate extinction and SERS EF, in a manner akin to plasmon sampled surface-enhanced Raman excitation profiles,[46] the extinction at 530 nm, corresponding to the midpoint between Raman excitation (514.5 nm) and scattered wavelengths (546.8 nm), is plotted versus the spacer SiO_2 thickness as displayed in Figure 4 b. It is interesting to see that the extinction profile tracks the SERS EF profile over the entire spacer range studied, with the peaks and valleys occurring at similar spacer

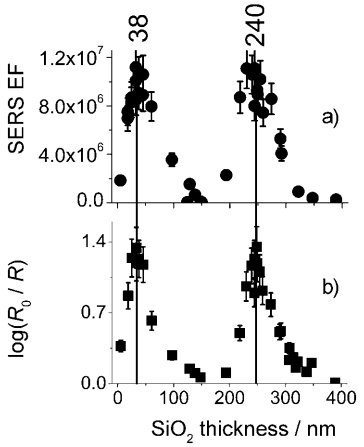

Figure 4. SERS EF vs SiO_2 thickness plot obtained with TE polarized 514.5 nm excitation a) for multilayer substrates having the same 6 nm AgIF thickness. Plot of extinction at 530 nm versus SiO_2 thickness (b) of multilayer substrates as in (a); 530 nm corresponds to the midpoint, $(\nu_{ex} + \nu_{Ram})/2$, between Raman excitation (514.5 nm) and scattered wavelengths (546.8 nm).

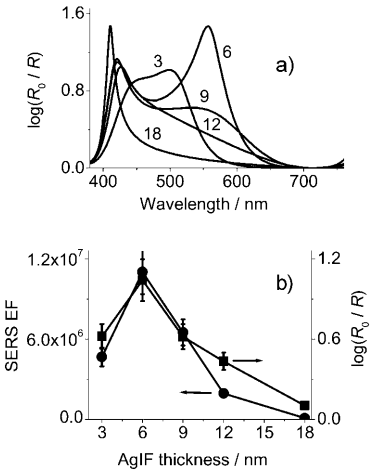

Figure 5. a) TE polarized extinction spectra of multilayer substrates, Ag(100)/SiO_2(250)/AgIF(xx), having the same 250 nm SiO_2 thickness but different thicknesses of AgIF. The number adjacent to the extinction spectrum corresponds to AgIF thickness in nanometers. b) SERS EF versus AgIF thickness (●) obtained by TE polarized 514.5 nm excitation, and extinction at 530 nm versus AgIF thickness (■) plots of the same substrates as in (a).

thicknesses. Similar extinction profile plots were obtained for both 514.5 and 546.8 nm. The maxima in the SERS EF occur in the spacer SiO_2 thickness regions 25–46 nm and 230–260 nm, where the extinction spectra have intense visible extinction and the minimum occurs in the spacer thickness region, 120–170 nm, where the extinction of the visible light is very weak.

In order to determine whether the SERS EF and extinction correlation holds for excitations other than 514.5 nm, the SERS EFs (of 1141 cm^{-1} band of NAB) of the multilayer substrates which has 6 nm AgIF are determined as a function of SiO_2 thickness with 647.1 nm excitation. As shown in Figure S2 (Supporting Information), a plot of SERS EF versus SiO_2 thickness with 647.1 nm excitation shows maxima at ~45 and ~307 nm SiO_2 thicknesses with SERS EFs of 2.1×10^7 and 3.4×10^7 respectively, and a minimum SERS EF of 1.1×10^4 at ~200 nm SiO_2. The spacer thickness modulates SERS EF by ~3,000. The plot of extinction at 672 nm [corresponding to $(\nu_{ex} + \nu_{Ram})/2$] versus SiO_2 thickness shows peaks at ~45 and ~307 nm and a minimum at ~200 nm confirming that SERS EF and extinction correlation is valid for 647.1 nm excitation. Furthermore, the SERS EF of Ag(100)/SiO_2(307)/Ag(6) substrate for 647.1 nm excitation is ~30 times larger than that observed for the same 6 nm AgIF on glass.

To investigate how AgIF affects the extinction spectra and SERS EFs of multilayer substrates, the thickness of AgIF is varied while keeping the spacer SiO_2 thickness constant. Figure 5a shows that a small change in the AgIF thickness at a constant spacer SiO_2 thickness has dramatic effect on the extinction spectrum. For example, changing AgIF thickness from 3 nm to 6 nm shifts the extinction maximum from 502 nm to 556 nm and in addition, the two spectra have very different lineshapes. The 6 nm thick AgIF has two distinct peaks compared to a single resolved peak for 3 nm AgIF. Increasing AgIF thickness beyond 6 nm leads to decrease in visible extinction, indicating that the SERS EF should decrease at larger AgIF thickness. Figure 5b shows the plot of SERS EF versus AgIF thickness determined by excitation with TE polarized 514.5 nm laser. The plot has a peak at 6 nm AgIF thickness (the reason why 6 nm AgIF is used for the study) with a SERS EF of ~1.1×10^7 and decreases by more than two orders of magnitude to 9.4×10^4 at 18 nm. The extinction AgIF thickness profile, that is, the plot of the extinction at 530 nm versus AgIF thickness, tracks the SERS EF thickness profile (Figure 5b) further indicating that the multilayer substrates modulate plasmons via the interference effect, and the plasmons in turn modulate the SERS EF. Increasing AgIF thickness corresponds to changing the morphology of AgIF and is clearly different from changing the spacer thickness.

An important question in the development of highly active SERS substrate is whether the multilayer substrate improves the SERS EF of the nanostructure compared to that of the same nanostructure on unlayered substrates such as glass. To answer this question, we examine the plasmon extinction spectra and SERS EFs of AgIF on a glass slide. As shown in Figure 6a, the plasmon resonance extinction spectra of different thicknesses of AgIF on glass recorded in the transmission mode varies strongly with AgIF thickness. The spectrum red-shifts, broadens, and the absorbance increases as the AgIF thickness increases from 3 to 9 nm. Further increase in thickness leads to increased broadening of the absorption spectrum with no peaks in the visible region. The broadening of the extinction spectrum with AgIF thickness can be understood as due to the combined effects of the increase in particle size, changes in particle shape due to coalescence of neighboring particles, and increase in interparticle coupling as the particles get closer. At thickness above 12 nm the particles begin to form an extended network of conducting particles or a continuous film.[47] The SERS EF versus AgIF thickness plot (Figure 6b) obtained on 514.5 nm excitation with glass as the substrate has a plateau value of ~1.1×10^6 at AgIF thickness region 6–9 nm and drastically decreases to 9.4×10^4 at 18 nm. This

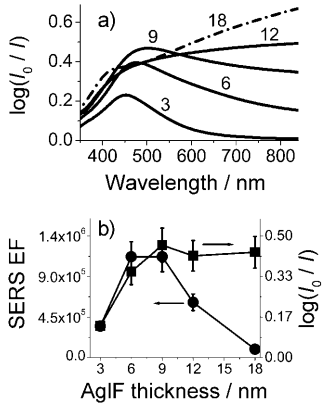

Figure 6. Absorption spectra of glass slides which have different thicknesses of AgIF recorded in transmission mode (a). Plots of SERS EF versus AgIF thickness (●) obtained by TE polarized 514.5 nm excitation, and extinction at 530 nm versus AgIF thickness (■) (b) of the same samples as in (a). The number adjacent to the absorption spectrum in (a) corresponds to AgIF thickness in nm.

shows that the SERS EF of AgIF on glass is an order of magnitude less than that of the corresponding AgIF on multilayer substrate which has the optimum spacer thickness. In the case of AgIF on glass substrate, a good extinction and SERS EF correlation was observed for AgIF thickness up to 9 nm. However, at higher thicknesses a significant deviation between extinction and SERS EF is observed, indicating the formation of non-SERS active nanostructures. A more detailed discussion on the possible reasons for the deviation can be found in Figure S3 (Supporting Information).

The SERS EFs from multilayer substrates at certain spacer SiO_2 thicknesses are an order of magnitude or more than that of highest SERS EF obtained from the unlayered glass substrates. The ratio of the SERS EF, multilayer substrate to glass, increases with decrease in Raman excitation frequency. For 514.5 nm excitation the ratio is ~10, and it increases to ~30 for 647.1 nm excitation. Since interference effect modulates the SERS EF of the multilayer substrate, there are maxima and minima in the SERS EF as the spacer SiO_2 thickness is varied. For example, with 514.5 nm excitation, maxima occur at 38 and 240 nm SiO_2 thicknesses with almost identical SERS EF of 1.1×10^7. A minimum occurs at 150 nm SiO_2 thickness with SERS EF of 4.8×10^4, and at this SiO_2 thickness the SERS EF of the multilayer substrate is ~20 times smaller than that of the unlayered glass substrate. Hence implementation of the multilayer substrate to benefit the enhanced SERS EF requires informed choice of the spacer thickness of the multilayer substrate and the Raman excitation frequency.

Tuning of the extinction spectra in multilayer substrates can have contributions from two effects: the interference effect and/or LSPR and SPP coupling. Coupling between LSPR and SPP propagating on the surface of a reflecting noble-metal layer is a near-field effect and is effective only at short distances.[31,39–42,48] The coupling strength between LSPR and SPP decreases exponentially with the separation distance and becomes negligible at a distance of a few particle diameter. Hence, the extinction spectrum due to LSPR–SPP coupling redshifts with decreasing distance which is contrary to the effect observed in the systems studied here. Leveque and Martin[40,41] showed that LSPR and SPP coupling is negligible at distances larger than 50 nm. In addition, gap plasmons are not expected to be important in the multilayer substrates studied here because of the large spacer thickness and the small size of the nanostructure.[36–38,49,50] Conclusive evidences that LSPR and SPP coupling is negligible at large spacer thickness is demonstrated by the fact that both the extinction spectra and SERS EFs are virtually unaffected when the reflecting Ag mirror of the multilayer substrate, $Ag/SiO_2/AgIF$, is replaced by Al, $Al/SiO_2/AgIF$, which is plasmon inactive in the visible region[51,52] as shown in Figure S4 (Supporting Information). This indicates that interference effect is the predominant contributor to the tuning of the extinction by multilayer substrates studied here.

As shown in Figure 2a and the Supporting Information (Figure S1), a strong correlation is observed between the extinction spectra of the multilayer substrates with and without AgIF indicating that interference effects modulate the spectra. This raises relevant questions on the role of AgIF in the spectral modulation. Is AgIF acting as a benign reflector that enhances the interference effect? Or does it act as an active component and the observed spectral modulation is due to the excitation of LSPR? An unambiguous answer to these questions is prevented by the broad extinction spectrum (Figure 1) of 6 nm AgIF on glass that spans the entire visible range. Therefore, polythiophene with relatively sharp absorption spectrum (with two unresolved peaks at 555 and 596 nm in the visible region) was used to determine how interference effects due to the multilayer substrate modulates the spectrum.

When a thin-film of polythiophene (~25 nm) is spin-coated on multilayer substrates which have different spacer thicknesses as in Figures 1and 2, tuning of the extinction intensity and spectrum of polythiophene is observed. It is important to note that the spectral tuning is confined within the absorption spectrum of polythiophene indicating that the function of the multilayer substrate is to tune the allowed vibronic transitions of polythiophene (details to appear in a separate communication). In addition, a strong correlation between extinction (at excitation wavelength) and Raman intensity is observed as in the case of AgIF on multilayer substrates. In the case of molecular resonances, when the excitation wavelength is resonant with a strongly allowed electronic excited state, the Raman scattering is dominated by Albrecht A-term. Under these conditions, both absorption and resonance Raman cross sections depend on the same excited state parameters and the strong correlation that exist between them is now well established.[53–55] It is important to note that polythiophene on multilayer substrate, with optimum spacer thickness to enhance the Raman signal, provides additional $>$10-fold Raman intensity enhancement compared to that on the glass substrate as in the case of AgIF.

There are fundamental differences between AgIF and polythiophene thin-films. The polythiophene extinction spectrum arises from electronic transitions between discrete energy levels of the molecule. On the other hand, the spectrum of AgIF is due to collective oscillation of free electrons called plas-

mons in the AgIF whose resonance frequency depends on the shape, size, particle spacing and relative orientations, and the dielectric environment. Another difference between molecular and plasmonic resonances is that the magnitude of polarization on plasmon excitation is much larger than the excitation of the molecular excited states. Hence any effect which depends on polarization is expected to be much more pronounced in metal nanostructures.

The experimental results shown above clearly indicate that the extinction spectra of AgIF on multilayer substrates are due to the excitation of plasmon resonances. Multilayer substrate tunes both the intensity and frequency of the extinction spectrum by simply changing the spacer layer thickness and consequently the SERS EF. This observation is similar to a recent report[56] on the reflectance spectra obtained from gold nanoparticles immobilized on porous Al_2O_3 of variable thickness prepared on a reflecting aluminum film. They attributed the observed reflectance to interference localized surface plasmon resonance. It is important to note that the extinction spectrum of AgIF, obtained by vacuum evaporation of Ag, is broad and spans the entire visible region corresponding excitation of multiple plasmon resonances of Ag nanostructures which have different sizes, shapes, relative orientations, and interparticle spacings. Changing the spacer layer thickness of the multilayer substrate allows selective excitation of a subset of these plasmon resonances in AgIF and it should be noted that this does not constitute tuning plasmon resonance as achieved by changing the shape and size of monodispersed Ag nanoparticles. A useful analog to the tuning observed here is the tuning of laser frequencies in a dye laser. In a dye laser, the tuning range of the laser is determined by the bandwidth of the dye fluorescence emission spectrum, and lasing at a particular wavelength can be achieved by placing a wavelength selective optical element such as, lyot filter, prism or grating in the optical cavity.

In a multilayer substrate, the light waves suffer multiple reflections and refractions at the interfaces. The dielectric layer thickness and the phase change at the interfaces modulate the phase, and interference at these interfaces modulates the intensity of the propagating light. As we have stated earlier,[35] changing the spacer thickness modulates the phase and mean square electric field of light propagating within the spacer layer which in turn modulates the extinction in the AgIF. Nanostructures are known to have very high extinction coefficients[57] for plasmon excitation. Plasmons are waves or coherent oscillations of free electrons in Ag nanostructures, and the plasmon interference effect[58–60] is now well documented. Hence, the plasmon interference effect is expected to play an important role in the observed extinction spectrum of AgIF on multilayer substrate. Contributions from plasmon interference may be responsible for the observed discrepancies between the experimental and simulated (using a commercially available optical thin-film software "FILMSTAR'' from FTG Software Associates) extinction spectra of AgIF on multilayer substrates (Supporting Information Figures S5 and S6). Raman and SERS intensities are proportional to E^2 and E^4 of the incident excitation electric field respectively. In spite of this difference both polythiophene and AgIF on multilayer substrates have similar ~10 fold additional Raman intensity enhancement compared to the unlayered glass substrates. These results show that the modulation of Raman intensity by the multilayer substrate is due to interference mediated tuning of the plasmonic and molecular resonances.

3. Conclusions

A multilayer substrate tunes both the intensity and frequency of the extinction spectrum of silver nanostructures that support multiple plasmon resonances. Multilayer substrates modulate the SERS EF of the AgIF by a factor of ~200 and ~3,000 for 514.5 and 647.1 nm excitations respectively, as the spacer dielectric-layer thickness is varied. At the optimum spacer thickness, multilayer substrates can provide more than an order of magnitude increase in the SERS EF for AgIF compared to that of the unlayered glass substrate. The additional order of magnitude SERS signal enhancement provided by the multilayer structures opens up a new possibility to further boost the Raman signals from any SERS active nanostructure. Future work in this line includes investigation of composite multilayer substrates with lithographically-fabricated nanostructure arrays which have well-defined shapes, sizes, spacings, and orientations.

Experimental Section

Multilayer substrates were fabricated on 13 mm x 18 mm thermally oxidized silicon wafers by electron beam evaporation (Johnsen Ultravac E-beam) at $\sim 10^{-6}$ torr of the following materials in succession: 5 nm adhesion Cr, 100 nm reflecting Ag, and variable thickness transparent SiO_2 spacer layers (all 99.99% pure from Kurt J. Lesker). Deposition rates monitored by a quartz crystal microbalance were 0.02–0.1 nm s^{-1} for the multilayer substrate, and < 0.02 nm s^{-1} for the SERS active AgIF.[35] Variable angle spectroscopic ellipsometry (J. A. Woollam Co., Inc.) was used to verify the SiO_2 thickness indicated by the quartz crystal balance during deposition. Transverse electric (TE) or transverse magnetic (TM) polarized UV/Vis extinction spectra were collected in an external reflection mode at 45° incident angle with a Perkin–Elmer Lambda 900 UV/Vis/NIR double beam spectrometer. The extinction refers to $\log(R_o/R)$, where R_o and R are the reflectance of the reference, Si/SiO_2/Cr(5)/Ag(100), and the sample, Si/SiO_2/Cr(5)/Ag(100)/SiO_2(xx)/AgIF, respectively. Coherent Ar ion laser and Chromex Raman spectrograph with an Andor CCD detector was used to excite, collect, disperse, and detect the Raman scattered light from the samples. As described in detail in a previous report,[35] multilayer substrates with SERS active AgIF were modified with nitroazobenzene (NAB) by immersing the freshly fabricated substrates in a 0.4 mM nitroazobenzene diazonium salt solution in acetonitrile for ~1 s.

Acknowledgements

The author thanks Professor Richard M. McCreery for his support, invaluable suggestions and discussions, and Prof. Anne M. Kelley, University of California, Merced for useful suggestions. This work was supported by the National Institute for Nanotechnology, and the University of Alberta. The National Institute for Nanotechnol-

ogy is operated as a partnership between the National Research Council and the University of Alberta and is jointly funded by the Government of Canada, the Government of Alberta, and the University of Alberta. A portion of this work was carried out at the University of Alberta Nanofab facility.

Keywords: interference · multilayer substrate · plasmon resonance · spacer · surface enhanced Raman scattering

[1] H. B. Akkerman, B. de Boer, *J. Phys. Condens. Matter* **2008**, *20*, 013001.
[2] R. L. McCreery, A. J. Bergren, *Adv. Mater.* **2009**, *21*, 4303.
[3] Y. Selzer, D. L. Allara, *Ann. Rev. Phys. Chem.* **2006**, *57*, 593.
[4] S. M. Lindsay, M. A. Ratner, *Adv. Mater.* **2007**, *19*, 23.
[5] A. P. Bonifas, R. L. McCreery, *Chem. Mater.* **2008**, *20*, 3849.
[6] A. M. Nowak, R. L. McCreery, *J. Am. Chem. Soc.* **2004**, *126*, 16621.
[7] J. Kneipp, H. Kneipp, K. Kneipp, *Chem. Soc. Rev.* **2008**, *37*, 1052.
[8] E. C. Le Ru, P. G. Etchegoin, in *Principles of Surface-Enhanced Raman Spectroscopy and Related Plasmonic Effects*, Elsevier, Amsterdam, **2009**.
[9] R. Aroca, in *Surface Enhanced Vibrational Spectroscopy*, Wiley, Hoboken, New Jersey, **2006**.
[10] S. M. Nie, S. R. Emery, *Science* **1997**, *275*, 1102.
[11] K. Kneipp, Y. Wang, H. Kneipp, L. T. Perelman, I. Itzkan, R. Dasari, M. S. Feld, *Phys. Rev. Lett.* **1997**, *78*, 1667.
[12] M. Moskovits, *Rev. Mod. Phys.* **1985**, *57*, 783.
[13] G. C. Schatz, M. A. Young, R. P. Van Duyne in *Surface-Enhanced Raman Scattering: Physics and Applications, Topics in Applied Phyiscs*, Vol. 103 (Eds.: K. Kneipp, M. Moskovits, H. Kneipp), Springer, Berlin, **2006**, p. 19.
[14] M. I. Stockman, *Surface-Enhanced Raman Scattering: Physics and Applications, Topics in Applied Phyiscs,* Vol. 103 (Eds.: K. Kneipp, M. Moskovits, H. Kneipp), Springer, Berlin, **2006**, p. 47.
[15] J. Zhao, J. A. Dieringer, X. Y. Zhang, G. C. Schatz, R. P. Van Duyne, *J. Phys. Chem. C* **2008**, *112*, 19302.
[16] A. D. McFarland, M. A. Young, J. A. Dieringer, R. P. Van Duyne, *J. Phys. Chem. B* **2005**, *109*, 11279.
[17] A. Campion, P. Kambhampati, *Chem. Soc. Rev.* **1998**, *27*, 241.
[18] A. Otto, M. Futamata in *Surface-Enhanced Raman Scattering: Physics and Applications, Topics in Applied Phyiscs,* Vol. 103 (Eds.: K. Kneipp, M. Moskovits, H. Kneipp), Springer, Berlin, **2006**, p. 147.
[19] H. Wang, D. W. Brandl, P. Nordlander, N. J. Halas, *Acc. Chem. Res.* **2007**, *40*, 53.
[20] S. Lal, N. K. Grady, J. Kundu, C. S. Levin, J. B. Lassiter, N. J. Halas, *Chem. Soc. Rev.* **2008**, *37*, 898.
[21] S. Eustis, M. A. El-Sayed, *Chem. Soc. Rev.* **2006**, *35*, 209.
[22] P. N. Njoki, I. I. S. Lim, D. Mott, H. Y. Park, B. Khan, S. Mishra, R. Sujakumar, J. Luo, C. J. Zhong, *J. Phys. Chem. C* **2007**, *111*, 14664.
[23] S. Lal, S. Link, N. J. Halas, *Nat. Photonics* **2007**, *1*, 641.
[24] C. L. Haynes, R. P. Van Duyne, *J. Phys. Chem. B* **2001**, *105*, 5599.
[25] L. R. Hirsch, A. M. Gobin, A. R. Lowery, F. Tam, R. A. Drezek, N. J. Halas, J. L. West, *Ann. Biomed. Eng.* **2006**, *34*, 15.
[26] N. R. Jana, L. Gearheart, C. J. Murphy, *J. Phys. Chem. B* **2001**, *105*, 4065.
[27] C. G. Khoury, T. Vo-Dinh, *J. Phys. Chem. C* **2008**, *112*, 18849.
[28] Y. G. Sun, Y. N. Xia, *Science* **2002**, *298*, 2176.
[29] J. Aizpurua, P. Hanarp, D. S. Sutherland, M. Kall, G. W. Bryant, F. J. G. de Abajo, *Phys. Rev. Lett.* **2003**, *90*, 057401.
[30] A. Leitner, Z. S. Zhao, H. Brunner, F. R. Aussenegg, A. Wokaun, *App. Optics* **1993**, *32*, 102.
[31] W. R. Holland, D. G. Hall, *Phys. Rev. Lett.* **1984**, *52*, 1041.
[32] H. G. Bingler, H. Brunner, A. Leitner, F. R. Aussenegg, A. Wokaun, *Mol. Phys.* **1995**, *85*, 587.
[33] J. P. Goudonnet, J. L. Bijeon, R. J. Warmack, T. L. Ferrell, *Phys. Rev. B* **1991**, *43*, 4605.
[34] W. S. Bacsa, J. S. Lannin, *App. Phys. Lett.* **1992**, *61*, 19.
[35] L. C. T. Shoute, A. J. Bergren, A. M. Mahmoud, K. D. Harris, R. L. McCreery, *App. Spect.* **2009**, *63*, 133.
[36] H. T. Miyazaki, Y. Kurokawa, *Phys. Rev. Lett.* **2006**, *96*, 4.
[37] D. K. Gramotnev, S. I. Bozhevolnyi, *Nat. Photon.* **2010**, *4*, 83.
[38] J. Jung, T. Søndergaard, S. I. Bozhevolnyi, *Phys. Rev. B* **2009**, *79*, 035401.
[39] P. Nordlander, E. Prodan, *Nano Lett.* **2004**, *4*, 2209.
[40] G. Leveque, O. J. F. Martin, *Optics Express* **2006**, *14*, 9971.
[41] G. Leveque, O. J. F. Martin, *Optics Lett.* **2006**, *31*, 2750.
[42] T. Okamoto, I. Yamaguchi, *J. Phys. Chem. B* **2003**, *107*, 10321.
[43] H. C. Kim, X. Cheng, *Optics Express* **2009**, *17*, 17234.
[44] L. P. Du, X. J. Zhang, T. Mei, X. C. Yuan, *Optics Express* **2010**, *18*, 1959.
[45] J. M. Montgomery, A. Imre, U. Welp, V. Vlasko-Vlasov, S. K. Gray, *Optics Express* **2009**, *17*, 8669.
[46] C. L. Haynes, R. P. Van Duyne, *J. Phys. Chem. B* **2003**, *107*, 7426.
[47] A. Anders, E. Byon, D. H. Kim, K. Fukuda, S. H. N. Lim, *Solid State Commun.* **2006**, *140*, 225.
[48] J. D. Driskell, R. J. Lipert, M. D. Porter, *J. Phys. Chem. B* **2006**, *110*, 17444.
[49] Y. Kurokawa, H. T. Miyazaki, *Phys. Rev. B* **2007**, *75*, 035411.
[50] T. Sondergaard, J. Jung, S. I. Bozhevolnyi, G. Della Valle, *New J. Phys.* **2008**, *10*, 105008.
[51] Y. L. Chen, Y. Fang, *Spectrochim. Acta A* **2008**, *69*, 733.
[52] Y. J. Mo, P. Wachter, U. Martin, F. K. Reinhart, *J. Phys. Chem. Solids* **1995**, *56*, 975.
[53] A. M. Kelley, *J. Phys. Chem. A* **1999**, *103*, 6891.
[54] L. C. T. Shoute, R. Helburn, A. M. Kelley, *J. Phys. Chem. A* **2007**, *111*, 1251.
[55] L. C. T. Shoute, G. R. Loppnow, *J. Chem. Phys.* **2002**, *117*, 842.
[56] H. M. Hiep, H. Yoshikawa, E. Tamiya, *Anal. Chem.* **2010**, *82*, 1221.
[57] J. Yguerabide, E. E. Yguerabide, *Anal. Biochem.* **1998**, *262*, 157.
[58] R. Zia, M. L. Brongersma, *Nat. Nanotechnol.* **2007**, *2*, 426.
[59] R. Kolesov, B. Grotz, G. Balasubramanian, R. J. Stohr, A. A. L. Nicolet, P. R. Hemmer, F. Jelezko, J. Wrachtrup, *Nat. Phys.* **2009**, *5*, 470.
[60] E. Altewischer, M. P. van Exter, J. P. Woerdman, *Nature* **2002**, *418*, 304.

Received: May 8, 2010
Revised: June 20, 2010
Published online on August 3, 2010

